Transient Polarization in Insulating CdS†

N. F. J. MATTHEWS* AND PETER J. WARTER, JR.‡
Princeton University, Princeton, New Jersey
(Received 8 September 1965)

Transient-current measurements have been carried out on single crystals of insulating CdS having noninjecting contacts. Application of step voltages to optically pre-excited crystals produced currents which lasted from 3000 sec and decayed as much as three orders of magnitude at temperatures in the neighborhood of 200°K. The total transported charge varied approximately as the square root of the applied voltage, suggesting that the crystal polarized with the formation of a positively charged cathode depletion layer produced by the thermal release of electrons from bound states. A description of the polarization process in terms of the dynamics of the formation of the cathode depletion layer is given, and a method for determining the concentrations, activation energies, and frequency factors of the trapping states taking part in the process is presented. For the crystals investigated the traps were found to lie at a single discrete energy level; the concentration of traps was $(2.5\pm1.5)\times10^{14}/cm^3$ and the activation energy was 0.63 ± 0.01 eV. The trapping cross section was found to be approximately 5×10^{-18} cm².

I. INTRODUCTION

INCREASING interest has been shown in the mechanisms which bring about the formation of space charge in insulators. An understanding of these mechanisms is essential in the study of dielectric breakdown, transport properties, characters of bound states, and injection of carriers through the cathodes of these materials. One scheme for investigating these mechanisms, which we have used with success, involves analyzing long-term polarization currents associated with one-carrier insulators having noninjecting contacts. Such currents arising in crystalline AgCl were observed and analyzed by Warter.[1] A theory which characterized the dynamics of depletion layer formation and which provided a method for determining certain properties of the bound states taking part in the process was developed and the theory was found to be in basic agreement with experimental results.

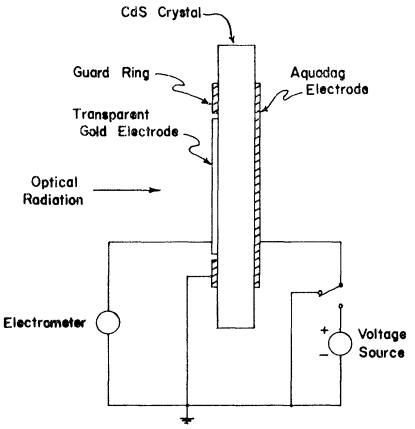

FIG. 1. Crystal electrode structure and external connections.

Similar measurements have been performed on insulating monocrystalline CdS. Cadmium sulfide was selected because its high photogain suggested that the free electron lifetime was much greater than the electron transit time and because a deeper understanding of the trapping properties of this material was desired.

II. TRANSIENT CURRENT MEASUREMENTS

The CdS crystals used in these experiments were platelets grown from the vapor phase by the method described by Bube and Thomsen,[2] which is a modification of the general method of Frerichs.[3] These crystals were *nominally pure* in that there was no intentional addition of impurities either during or after growth. All of the measurements were made on crystals from one batch grown at the RCA Laboratories. The crystals exhibited a photosensitivity intermediate between the extremes frequently observed in nominally pure CdS. A typical crystal was 1 mm×0.5 mm×40 μ thick. Aquadag was used for one of the noninjecting contacts and as an adhesive to attach the crystal to a sapphire mounting block. The other noninjecting contact was a transparent gold layer through which the crystal was photoexcited. Aquadag was also used to form a guard ring surrounding the gold contact. The geometric capacitance of the samples was between 0.5 and 1 pF. Figure 1 illustrates the electrode configuration and the connections to the vibrating reed electrometer and the battery voltage source.

Measurements were made on each sample until either the Aquadag holding the sample to the sapphire or one of the contact connections failed because of the repeated thermal cycling. A significant amount of data was obtained before failure on about ten samples. There was no significant difference in the nature of the data obtained, or in the interpretation of the data, for any of these samples. For this reason, the data presented are from only one sample, the one which yielded the widest range of data before failure. The variations from sample

† This work was supported in part by the U. S. Atomic Energy Commission. Use was made of computer facilities supplied in part by a grant from the National Science Foundation: NSF-GP579.
* Present address: North Carolina State University, Raleigh, North Carolina.
‡ Present address: Xerox Corporation, Rochester, New York.
[1] P. J. Warter, Jr., Ph.D. dissertation, Princeton University, 1962 (unpublished).
[2] R. H. Bube and S. M. Thomsen, J. Chem. Phys. **23**, 15 (1955).
[3] R. Frerichs, Phys. Rev. **72**, 594 (1947).

to sample in this batch of crystals is of the same order as the variation from one side to the other for the sample reported.

The crystals were optically pre-excited with a mercury arc lamp. Although illumination for several milliseconds was sufficient to fill the traps, the crystals were illuminated for several minutes to allow the lamp to stabilize so that the current measurements would be more reproducible from run to run. The voltage was not applied for 5 min after the arc lamp was shut off to allow the thermal afterglow in the lamp to extinguish completely and to allow the electronic traps with trap release times too short to be measured with this equipment to be completely emptied.

The sample holder was part of a thermal circuit which could be used to maintain the sample temperature constant to within 0.1°K at any temperature between 85°K and room temperature. Within this temperature range, significant polarization currents were observed only between 185 and 220°K. At temperatures below this range the currents were too small to measure reliably. At temperatures above this range the currents decayed too rapidly to be measured with the apparatus used. The fact that significant polarization currents were observed only over such a narrow range in temperature indicated that there was a significant density of trapping states at or near only one energy.

A. Square-Wave Response

In order to establish the character of the transient currents which arose during the polarization process, a square wave voltage of 500-sec half-cycle period was applied to the crystal starting five minutes after the end of the optical excitation. Figure 2 shows currents observed for the first two half-cycles in a typical case. The solid curve is the current which existed in the sample after it had been optically excited and the dashed curve is that in the same sample when unexcited. The effect of the optical excitation could be removed between runs, if desired, by warming the sample to room temperature and then recooling it to the temperature of the experiment while keeping the sample in the dark.

The time dependence of the currents observed in the dark as shown in Fig. 2 results from the fact that the square-wave voltage was put through a filter with a five-second rise time to prevent the initial charging current from overloading the electrometer. In this way, it is possible to integrate the current to get the true total charge transported in response to the change in voltage. The charge transported in the case of the unexcited sample is temperature-independent, linear with voltage, and agrees well with the charge one would expect on a CdS capacitor with the dimensions of the sample used. The charge transported is the same for either polarity and is twice as large on a voltage reversal as on an initial application of the same voltage. In short, the unexcited sample behaves as a simple capacitor.

Since the electrodes do not permit electrons to enter the bulk of the crystal, the fact that the charge transported in the pre-excited sample is much larger than the charge necessary to charge the electrodes indicates that there is electron transport in the bulk of the crystal. The fact that the currents persist in the optically pre-excited samples for thousands of seconds at the lower temperatures and the fact that the currents and the current decay rate are strong functions of temperature indicate that the electrons normally reside in bound states. What is observed is the drift of electrons with the field as they are thermally released from traps. Since the contacts are noninjecting, the free carriers (which we assume to be electrons) drift away from the negative electrode leaving a positively charged depletion layer adjacent to the cathode. The transient currents then monitor this process of depletion layer formation.

The current of the second half-cycle exhibits the same general character as that of the first, suggesting repolarization of the crystal as the result of the formation of another sheath adjacent to the opposite electrode. The currents observed during subsequent half-cycles are also similar to that of the first; they exhibit the long transient decay to negligibly small values. Figure 3 shows a plot of the charge transported during each half-cycle as a function of the half-cycle number. Since the current decays to a negligibly small value by the end of each half-cycle, the trapping states which take part in the process are almost completely empty by the end of each half-cycle. *If the thermal release of electrons from these same states is to account for the very similar transient current following the next application of a voltage of the same polarity, then electrons must be retrapped by these states during the next half-cycle while the sheath is forming at the opposite electrode.* The fact that the polarization currents continue on for many half-cycles is evidence that the probability of retrapping

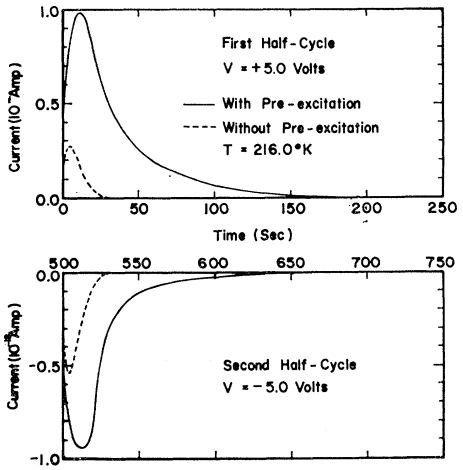

FIG. 2. Currents observed during the first cycle when a square-wave voltage is applied to the crystal.

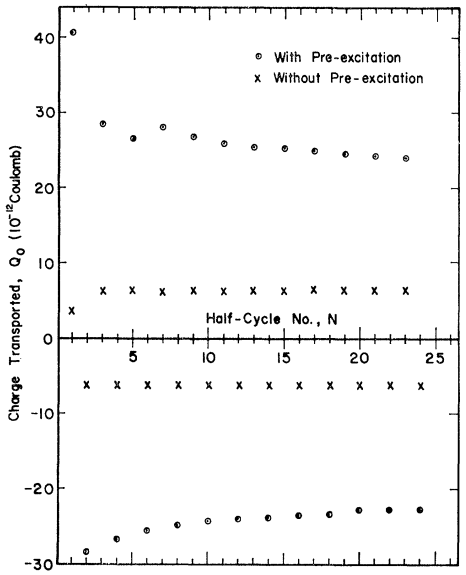

FIG. 3. Plot showing the slow decay of total transported charge with half-cycle number.

is far greater than the probability of recombination. The slow decay of the transported charge from cycle to cycle as shown in Fig. 3 is a measure of the rate of recombination.

B. Voltage Dependence of the Transported Charge

Further evidence for positive sheath formation adjacent to the noninjecting cathode may be obtained by considering the way in which the total transported charge depends on the magnitude of the applied voltage. If the charge density within the sheath is uniform, then the total polarization charge should vary as the square root of the voltage. Figure 4 shows a plot of the transported charge as a function of voltage in a typical case. The sample was held at a constant temperature (196.2°K) during these measurements. The crystal was re-excited with the mercury lamp prior to each transient current measurement. The total charge for both polarities of applied voltage are nearly, although not exactly, square root functions of the applied voltage. For comparison, the dashed line in Fig. 4 shows an ideal square-root dependence. The solid line in Fig. 4 is just the charge required to charge the unexcited sample.

The existence of the cathode sheath means that the electric field is concentrated in a small region of the sample with a maximum value at the cathode. One might thus expect breakdown at the cathode for large applied voltages. For voltages larger than 20 V, steady currents with a great deal of noise have indeed been observed.

The fact that the transported charge is different for the two polarities of voltage is an indication that the density of initially filled traps is different in the vicinity of the two electrodes. This was also indicated in Fig. 3 which shows that the charge transported in the first half-cycle is considerably greater than that in the second and subsequent half-cycles. The asymmetry does not continue for the later half-cycles since the total charge in the sample is limited to that in the depletion layer with the highest charge density. A set of measurements similar to those presented in Fig. 3 but with a negative voltage applied for the first half-cycle is consistent with this interpretation. In this case an unusually large charge is transported on the second half-cycle, i.e., the first positive half-cycle. All of the indications are that, for this sample, the trap density is twice as great near one electrode as near the other. In addition, if a critical field near the cathode is responsible for the departure from a linear dependence of $\log Q_0$ on $\log V_0$, then this departure should occur at some critical Q_0 since the electric field at the cathode is proportional to the transported charge. This is consistent with our experimental results on the breakdown.

C. Temperature Dependence of the Transported Charge

Further information about the polarization process and the trapping states involved can be obtained by considering the transient currents observed at different temperatures. Figure 5 shows a plot of log current versus time at several temperatures. The crystal was optically pre-excited at each temperature for a period of several minutes, ending 5 min before the application of the voltage (the $t=0$ time in Fig. 5).

The currents observed at each temperature are decidedly nonexponential functions of time. The rate of decay of the currents is seen to increase as the temperature increases. This is the behavior one would

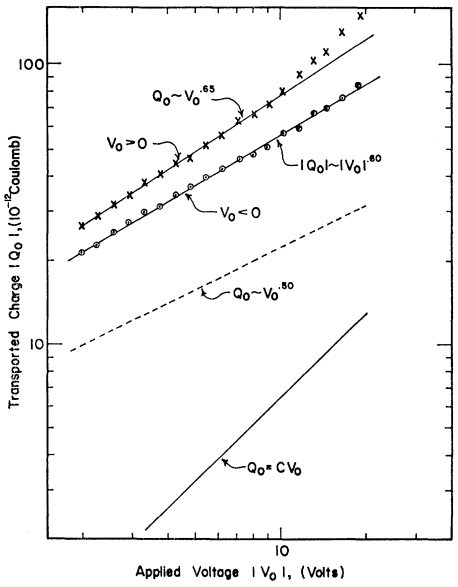

FIG. 4. Variation of transported charge with applied voltage.

expect if the thermal release of electrons from trapping states is the rate-limiting process. At the lower temperatures the rate of release of electrons from traps is small; hence, the formation of the cathode sheath is slow and the associated current, although small, decays slowly. At the higher temperatures the trap release time is short and the sheath forms quickly. The currents observed for a negative applied voltage are quite similar.

Figure 6 shows the total charge transported in the first 2000 sec after the application of the voltage as a function of temperature. Again the asymmetry between positive and negative voltages is apparent. At the higher temperatures, the transported charge is essentially independent of temperature indicating that a fixed number of trapping states takes part in the process. The charge drops off somewhat at the lower temperatures since, in these cases, there are still reasonable numbers of electrons remaining in traps after 2000 sec.

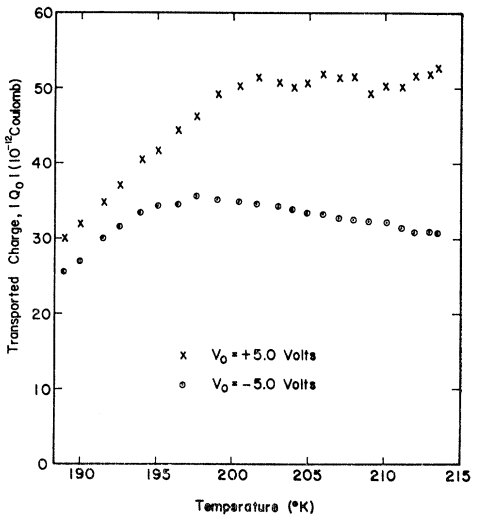

FIG. 6. Variation of total transported charge with temperature.

III. TRANSIENT DEPLETION-LAYER FORMATION

The experimental results presented above suggest that the transient currents observed in the optically pre-excited CdS crystals with noninjecting contacts monitor the formation of a depletion layer adjacent to the contact. In this section the theory appropriate to describe this sheath buildup is presented.

There are two different ways in which a depletion layer can form in an insulator where the charge carriers which ultimately leave the sheath region are initially in traps. An important parameter in distinguishing the two modes of sheath formation is the free carrier range. The range r is defined as the distance a free carrier travels per unit electric field from the point where it is thermally excited from the trap until it recombines or falls into a trap deep enough to remove it from the conduction process for a time significant in the particular experiment. Roughly, this means until the electron recombines or until it falls into a trap as deep or deeper then the one from which it was released. As discussed in the preceding section, retrapping by the same type of center as that from which the electron came is the dominant range-limiting process in the experiments with CdS being reported. It is sometimes convenient to think of the range as the product of the mobility and a free lifetime.

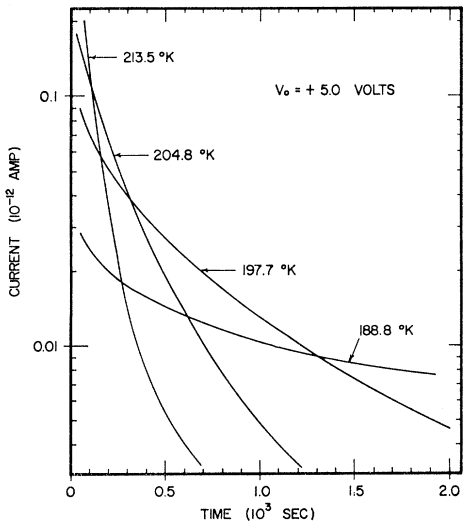

FIG. 5. Transient currents observed at several temperatures for a positive step voltage applied.

In order to classify the sheath formation processes, consider an optically pre-excited sample with no space charge to which a voltage is first applied at time, $t=0$. Suppose that only one type of carrier (electrons) contributes to the conduction current. The electrons are mainly in traps from which they are released at a finite, but low, rate and to which they return at approximately the same rate. As soon as the voltage is applied a positive space charge (of trapped holes) begins to form in a region of width, $X_c=rV_0/L$, adjacent to the cathode. V_0 is the applied voltage and L is the sample thickness. A long time after the voltage is applied to the sample, a steady-state depletion layer will form which has a width, $X_0=(2\epsilon V_0/en_t)^{1/2}$, where ϵ is the permittivity, e the electronic charge, and n_t the density of traps initially filled.

The two cases of depletion layer formation are the one for which $X_c/X_0<1$ and that for which $X_c/X_0>1$. The first case corresponds to the situation in which the sheath grows out from the cathode to a final width, X_0. The second case is that in which the sheath shrinks from a larger width towards X_0. These will be called the *short-* and *long*-range cases, respectively. The short-range case has been investigated by von Hippel *et al.*[4]

[4] A. von Hippel, E. P. Gross, J. G. Jelatis, and M. Geller, Phys. Rev. **91**, 568 (1953).

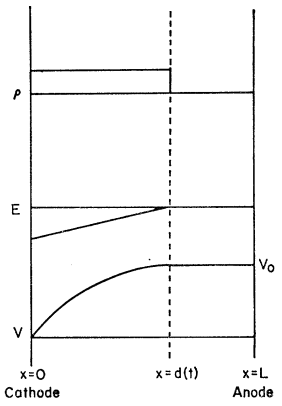

FIG. 7. Profiles of charge density, electric field, and potential after the sheath is well formed.

and is not the case of interest here. In the short-range case, the magnitude of the currents at different voltages is a linear function of the voltage, but the time scale varies as the square root of the voltage. This does not correspond to the currents observed in CdS. Furthermore, this model would not be expected to apply since CdS was chosen for these experiments because of its high photogain.

A. The Long-Range Model of Sheath Formation

In the case of an electron range sufficiently large that $X_c/X_0>1$, a positive sheath of width X_c begins to form adjacent to the noninjecting cathode immediately after the voltage is applied. After the net charge density in the sheath increases to the point that a major fraction of the applied voltage is dropped in the dipole layer formed by negative charges on the cathode and the positive charges distributed in the cathode sheath, the width of the cathode sheath will contract as the charge density in the sheath increases further.

The simplest situation to analyze is that in which the process of sheath formation has progressed to the point that nearly all of the applied potential drop is concentrated in the sheath region. If $X_c/X_0\gg1$, this will happen in a time that is short compared to the time constant for the thermal release of the trapped electrons. In this simple model the net charge density within the sheath is taken to be uniform and that outside the sheath to be zero. The sheath boundary is assumed to be well defined. In addition, the entire applied voltage is assumed to be across the dipole layer formed by the positive charges distributed uniformly in the sheath and the matching negative charges on the cathode.

Figure 7 illustrates the profiles of charge density, electric field, and potential across the sample. As electrons are released from traps within the sheath, they are quickly swept toward the anode under the influence of the electric field in the sheath region. As electrons leave the sheath, the net density of positive charge in the sheath region increases. Since the total potential drop across the sheath cannot exceed the applied voltage, the width of the sheath must decrease. A fraction of the electrons released within the sheath are retrapped at the sheath edge where they serve to neutralize the positive charge density. The remainder drift across the charge-free region and either leave the crystal at the anode or accumulate in a layer very close to the anode. In this simple model the field required to pull electrons across the charge-free region to the anode is assumed to be negligibly small, i.e., to make a negligible contribution to the total potential drop.

The equations which characterize sheath formation in this model can be determined easily. Integration of Poisson's equation using the boundary conditions, $V(0)=0$, $V(d(t))=V_0$, and $E(d(t))=0$, gives

$$V_0=\rho(t)d(t)^2/2\epsilon, \tag{1}$$

where $\rho(t)$ is the net positive charge density in the sheath and $d(t)$ is the sheath width. The total charge per unit area in the sheath is

$$q(t)=\rho(t)d(t). \tag{2}$$

Eliminating $d(t)$ from Eqs. (1) and (2) gives

$$q(t)=(2\epsilon V_0\rho(t))^{1/2}. \tag{3}$$

The conduction current density is

$$J(t)=\frac{dq(t)}{dt}=\left(\frac{\epsilon V_0}{2\rho(t)}\right)^{1/2}\frac{d\rho(t)}{dt}. \tag{4}$$

Combining Eqs. (3) and (4) gives

$$d\rho(t)/dt=q(t)J(t)/\epsilon V_0. \tag{5}$$

Equation (5) shows that if the conditions are such that this simple model is appropriate, then the transient current data can be used to study directly the release

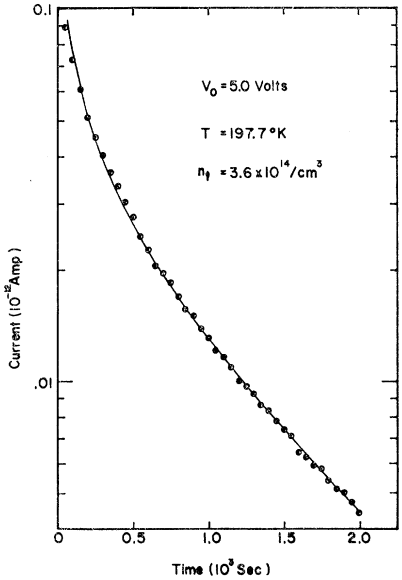

FIG. 8. Plot showing the close agreement between the observed current and the theoretical current of the simple model.

of electrons from traps. Of particular interest is the case where there is only one type of trap at one discrete energy. In this case the population of filled traps decreases exponentially with time. The rate of buildup of charge density within the sheath is then

$$\frac{d\rho(t)}{dt}=\frac{en_t}{\tau_t}\exp\left(\frac{-t}{\tau_t}\right). \tag{6}$$

In Eq. (6) n_t is the density of filled traps at time $t=0$, the time at which the voltage is applied, and τ_t is the trap release time which may be expressed as

$$1/\tau_t=\nu_t^*\exp(-E_t/KT). \tag{7}$$

Here E_t is the thermal activation energy of the trap species and ν_t^* is the trap *frequency factor* which characterizes the coupling between the lattice vibrations and electrons in traps. The current density predicted by the simple model in this case of one type of trap with a discrete activation energy is then

$$J(t)=\left[\frac{\frac{1}{2}\epsilon V_0 en_t}{1-\exp(-t/\tau_t)}\right]^{1/2}\frac{\exp(-t/\tau_t)}{\tau_t}. \tag{8}$$

Figure 8 shows a plot of the current data in one representative case. This current curve shows a consistent curvature and is obviously not exponential. The solid curve in Fig. 8 is the current predicted by the simple model for the case of the single trap species with the time constant and amplitude factor (τ_t and n_t) chosen so as to best fit the experimental data. It is evident from an inspection of Fig. 8 that the agreement in form between the data and the simple model for this case is excellent.

Figure 9 shows a semilogarithmic plot of a function proportional to the product of the current and the transported charge—the integral of the current from the time the voltage is applied—for the same current data presented in Fig. 8. The function $F(t)$ plotted in Fig. 9 is defined as

$$F(t)=I(t)\int_0^t I(t')dt'/\epsilon V_0 A^2, \tag{9}$$

where A is the electrode area. A comparison of Eqs. (5) and (9) shows that, if this model of sheath formation describes the observed transient polarization currents, there is a direct correspondence between $F(t)$ and $d\rho(t)/dt$.

The linear character of this semilog plot for times greater than 400 sec from the application of the voltage clearly suggests that electrons from one type of trap are responsible for the kinetics of the sheath formation. It is possible to determine directly from data such as those shown in Fig. 9 the density of filled traps and the time constant for the thermal release of electrons from the traps. Note that if the short-range case of sheath formation were the appropriate case, then neither the transient current nor $F(t)$ would have anywhere near the functional forms exhibited in Figs. 8 and 9.

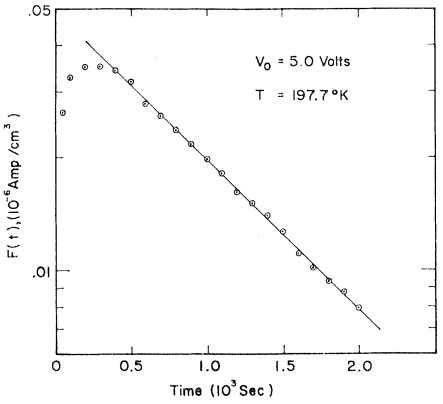

FIG. 9. Plot showing the slow rise and subsequent exponential decay of $F(t)$.

B. The Initial Stages of Sheath Formation—Determining the Electron Range

It is obvious from an inspection of Fig. 9 that the simple model is not adequate in this case for times less than 400 sec. The duration of the initial period during which $F(t)$ is not a decaying exponential function of time depends on the voltage and the temperature. This initial period is shorter at higher temperatures and at higher voltages. In the *long-range* model for sheath formation, the maximum sheath width is limited to $X_c=rV_0/L$. Thus, in the early stages of sheath formation, the voltage drop across the sheath will be significantly less than the applied voltage. This condition persists until the charge density within the sheath has time to build up.

It is possible to define a sheath formation time, T_s, with the following equation:

$$\rho(T_s)=2\epsilon V_0/X_c^2. \tag{10}$$

Substituting for X_c gives

$$\rho(T_s)=2\epsilon L^2/r^2V_0. \tag{11}$$

If the electrons are stored in a single type of trapping level and if $T_s<\tau_t$ for this level, then $\rho(T_s)\approx en_tT_s/\tau_t$. Making this approximation in Eq. (11), we obtain

$$T_s\approx 2\epsilon L^2\tau_t/en_tr^2V_0. \tag{12}$$

We assume that the peak in the curve of $F(t)$ occurs approximately at the sheath formation time, T_s. For the case presented in Fig. 9, the peak in $F(t)$ occurs approximately 250 sec after the voltage is applied. Using this value for T_s and extrapolating the exponential portion of the curve of $F(t)$ back to zero time to obtain a value for en_t/τ_t, we can obtain an estimate for the range from Eq. (12). This procedure gives $r\approx 0.6\times10^{-6}$ cm^2/V. This value is within the range of values ob-

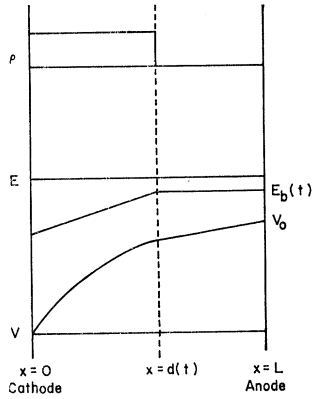

FIG. 10. Profiles of charge density, electric field, and potential for the range-limited model.

tained by van Heerden[5] in his pulsed measurements of the primary photocurrents in CdS. Although van Heerden's measurements were made on a much shorter time scale, and a correspondingly higher temperature, the similarity in the values obtained for the range suggests that the range-limiting process may be the same in the two cases.

It is possible to extend the simple model to describe the polarization during the initial stages of sheath formation. This *range-limited* model retains the assumption that the charge density within the cathode sheath is uniform, but it accounts for the nonnegligible electric field in the charge-free region outside the sheath region. Figure 10 illustrates the charge density, electric field, and potential profiles across the sample for this model. Except for the bulk field, Fig. 10 is essentially the same as Fig. 7 which illustrates the conditions in the simple model.

The sum of the voltage drops due to the bulk field, $E_b(t)$, and that due to the sheath dipole must equal the applied voltage:

$$\rho(t)d(t)^2/2\epsilon - E_b(t)L = V_0. \tag{13}$$

The conduction current density in the bulk (outside the sheath region) is equal to the rate of change of the total charge in the sheath:

$$J(t) = -[d(\rho(t)d(t))]/dt. \tag{14}$$

The conduction current density in the bulk is also equal to the product of the conductivity in the charge-free region and the bulk electric field $E_b(t)$. Since electrons are retrapped by the same type of centers, the density of electrons in traps in the bulk does not change with time. This means that the free-electron density in the bulk does not change with time. This is true, of course, only to the extent that electrons are not permanently lost because of recombination. As indicated in the preceding section, this is a good approximation for times quite long compared to the duration of the transient polarization current measurements in CdS since the recombination rate is at least several orders of magnitude less than the retrapping rate. The conductivity is just the product of the rate of release of electrons from traps, the electron range, and the electronic charge. If the density of traps and the type of traps are uniform throughout the sample, then the conductivity is uniform. The conduction current is then

$$J(t) = \sigma E_b(t) = (en_t r/\tau_t)E_b(t). \tag{15}$$

Equations (13), (14), and (15) may be combined to give an equation for the sheath width, $d(t)$:

$$\frac{\tau_t L}{en_t r}\frac{d(\rho(t)d(t))}{dt} + \frac{\rho(t)d(t)^2}{2\epsilon} = V_0. \tag{16}$$

This equation differs from the simple model by the inclusion of the term involving the electron range. Unfortunately, Eq. (16) is a nonlinear differential equation which has not been amenable to solution in closed form. A numerical solution has been obtained for a number of choices of the parameters. If everything but the range is assumed to be known from an analysis of the data in terms of the simple model, then the solutions to the polarization problem defined by Eq. (16) can be fitted to the $F(t)$ versus time data using the range as an adjustable parameter. The result of the best fit to the data presented in Fig. 9 is shown in Fig. 11. The value of the range which gives the best fit is $r = 0.7\times10^{-6}$ cm^2/V which is in excellent agreement with the approximate value determined by equating the time at the peak in the $F(t)$ versus time curve with the sheath formation time T_s defined by Eq. (12).

It is of interest to compare the initial sheath width X_c and the final sheath width X_0 for the results obtained above. Taking the relative dielectric constant[6] for CdS as 11.6, we obtain $X_c/X_0 = 2.4$ for $V_0 = 5.0$ V. This verifies the previous statement that the range is sufficiently large to place the sheath formation in the category of a shrinking sheath.

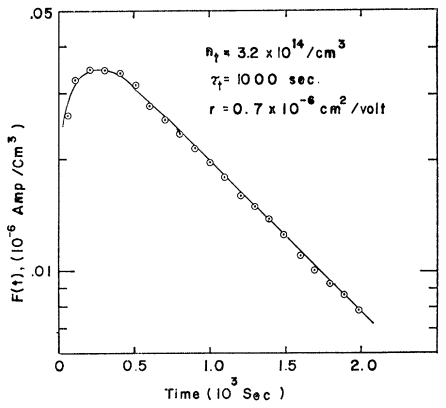

FIG. 11. Plot showing the close agreement between the observed current and the theoretical current of the range-limited model.

[5] P. J. van Heerden, Phys. Rev. **106**, 468 (1957).

[6] F. A. Kroger, H. J. Vink, J. Volger, Phillips Res. Rept. **10**, 39 (1955).

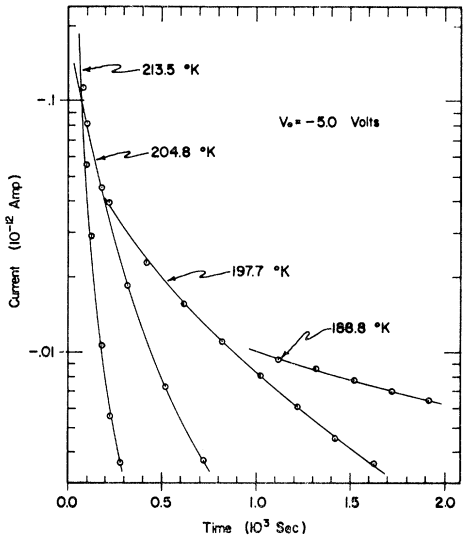

FIG. 12. Comparison of observed current with current of the simple model at several temperatures.

IV. TEMPERATURE DEPENDENCE OF τ_t

The above comparisons of experimental results with both the long-range model and the range-limited model agree with the assertion that a discrete trapping level is the primary source of electrons in the polarization process for the CdS crystals investigated. Further evidence of this is obtained from a consideration of the temperature dependence of the time constant, τ_t, characterizing the release of electrons from these traps. If a discrete level is the source of electrons, then τ_t should vary exponentially with inverse temperature according to Eq. (7), which may be written

$$\tau_t = (1/\nu^*) \exp(E_t/KT). \tag{17}$$

A plot of $\log \tau_t$ versus $1/KT$ should yield a straight line. From this straight line, the activation energy E_t and the frequency factor ν^* associated with the trap level may be determined.

Transient currents were recorded at intervals of approximately 1°K between 188 and 214°K. In each experiment the crystal was illuminated for 10 min with its electrodes shorted and then left in the dark for 5 min. A step voltage having a magnitude of 5.0 V was applied and the current was recorded for 2000 sec. The plots of Fig. 5 are typical of the currents observed.

The value for τ_t associated with each transient current was obtained by fitting the current of the simple model to the observed current. The charge density, $\rho(t)$, within the sheath was assumed to have the form of the first integral of Eq. (6). The time interval over which the fitting procedure was performed was selected to coincide with the interval over which the long-range model was believed to apply. The lower limit of the interval was taken as the time at which $F(t)$ as constructed directly from experimental data reached its maximum value. The upper limit of the time interval was 2000 sec or the time at which the current became lower than 3×10^{-15} A. Currents below this value were believed to have appreciable error since they corresponded to the lower 10% region of the lowest range of the electrometer used in taking the measurements.

A comparison of the theoretical currents of the simple model with several currents observed experimentally for $V_0 = -5.0$ V is shown in Fig. 12. The theoretical curves are computed from Eq. (4) with n_t and τ_t assigned the values of best fit. Each experimental current actually consists of approximately 650 data points distributed uniformly over the 2000-sec interval; for clarity, Fig. 12 shows a small fraction of the data points. The theoretical curves show close agreement with experimental results over the respective intervals of interest.

At each temperature the value of best fit for the initial concentration of electrons in traps lies within a factor of two of the value, $n_t = 2.0\times10^{14}/\text{cm}^3$. This value of n_t agrees closely with the value obtained from the plot of Fig. 6. From that plot the total transported charge, $|Q_0|$, for a well-formed sheath is approximately 3.2×10^{-11} C. Substituting this value into Eq. (3) yields $n_t = Q_0^2/(2\epsilon V_0 e A^2)$ or $n_t = 1.2\times10^{14}/\text{cm}^3$. The electrode area and the permittivity have the values, $A = 2.3\times10^{-3}$ cm^2 and $\epsilon = 1.03\times10^{-12}$ F/cm, respectively.

The temperature dependence of τ_t is shown in Fig. 13, where $\log \tau_t$ is plotted versus $1/KT$. For the negative case $\log\tau_t$ changes linearly with $1/KT$ over almost two orders of magnitude of τ_t. This behavior lends further credence to the belief that trapping states located at a discrete level are the primary source of electrons during the polarization process. The activation energy and

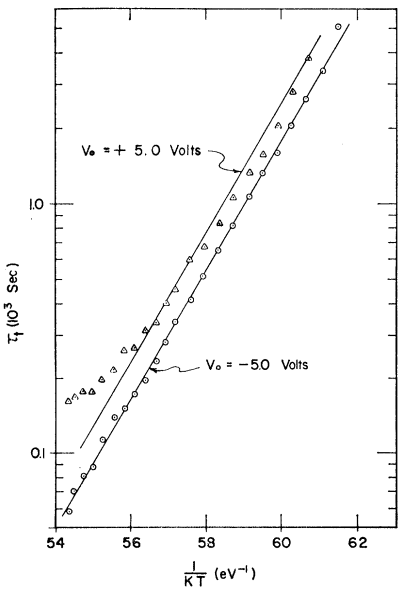

FIG. 13. Temperature dependence of τ_t.

the frequency factor characterizing the trapping level may be obtained by fitting the straight line of Eq. (17) to the series of points. The values of E_t and ν^* which provide the best fit for the negative voltage case are $E_t=0.63$ eV and $\nu^*=0.97\times10^{13}$/sec. Thus, the trapping level lies deep within the forbidden gap as we would expect.

The choice of a criterion for estimating the errors in E_t and ν^* must be somewhat arbitrary since the points which make up the plot depend upon such factors as the time interval for which the fitting procedure is carried out and the degree to which the long range model describes the process in the interval. A good estimate for the errors may be found by assuming the points to be distributed normally about the line of best fit and by determining the limiting values of E_t and ν^* which correspond to the 90% confidence limits. Such an analysis yields values for the errors

$$\Delta E_t=0.01 \text{ eV} \quad \text{and} \quad \Delta\nu^*=0.40\times10^{13}/\text{sec},$$

where it is assumed that the points are distributed according to Student's "t" distribution. Thus, the activation energy may be considered correct to within 2% and the frequency factor correct to within a factor of two.

For the positive voltage case, $\log\tau_t$ increases linearly with $1/KT$ except for the lower values of $1/KT$. Even though the time constant is consistently larger than that for the negative voltage case at all temperatures, the slopes of the plots are in close agreement. The differences in the values of the time constants and the departure from the linear dependence of $\log\tau_t$ upon $1/KT$ at the lower values of $1/KT$ for the positive voltage case are likely due to trapping states which lie at levels other than the discrete level of interest. Certainly, larger numbers of electrons are liberated when the positive voltage is applied (see Fig. 6). A fraction of these electrons may well come from states having different properties which can serve to effectively increase the time constant of interest.

V. DETERMINING THE TRAPPING CROSS SECTION

Knowledge of the value of the frequency factor associated with the discrete trapping level allows us to obtain an estimate for the capture cross section of these states. The trapping cross section σ_t for electrons is

$$\sigma_t=[\tau_c v_t(N_t-n_t)]^{-1}, \tag{18}$$

where v_t is the average thermal velocity of electrons, N_t is the concentration of trapping states at the discrete energy level, and τ_c is the average time an electron remains in the conduction band before being trapped. Equation (18) relates to conditions in the bulk of the crystal where the concentration n_t of electrons residing in traps is known.

The average thermal speed of free electrons is

$$v_t=(3KT/m^*)^{1/2}, \tag{19}$$

where m^* is the effective mass for the electron. With the assumption that the crystal is in quasithermal equilibrium, the concentration of empty states, N_t-n_t, is related to the frequency factor by

$$N_t-n_t=N_c/\tau_c\nu^*, \tag{20}$$

where N_c is the effective density of states in the conduction band. The quantity N_c is given by

$$N_c=2(2\pi m^*KT)^{3/2}/h^3, \tag{21}$$

where h is Planck's constant.

Eliminating N_t-n_t from Eq. (18) yields

$$\sigma_t=\nu^*/(v_tN_c). \tag{22}$$

Taking the effective mass[7] of the electron as 0.16 times the rest mass and T as 200°K (a midrange temperature for the experiments performed) gives $v_t=2.5\times10^7$ cm/sec and $N_c=9\times10^{17}$/cm^3. From the previous section the frequency factor has the value, $\nu^*=10^{13}$/sec. Substitution of these values into Eq. (22) gives the trapping cross section the value

$$\sigma_t=5\times10^{-13} \text{ cm}^2.$$

Thus, as we would expect, the trapping cross section is quite large. We also expect that the recombination cross section is significantly smaller than this as suggested by previous experimental results (see Fig. 3).

The fraction of trapping states which are filled is also of interest. Rewriting Eq. (20) yields

$$\frac{n_t}{N_t}=[1+\mu N_c/(rn_t\nu^*)]^{-1}, \tag{23}$$

where τ_c is replaced by r/μ. Taking the mobility[8] as large as 600 cm^2/V sec and substituting for the known quantities in Eq. (23) yields the result $n_t/N_t=0.6$. Thus, a large fraction of the trapping states are filled. This means that the quasifermi level lies very near the discrete trapping level as we might expect.

VI. THE DOUBLE SHEATH

We have stated that a stationary positively charged sheath exists adjacent to the cathode after all electrons initially in traps in the sheath region have been released and swept out of the crystal by way of the anode. If at this time the polarity of the applied voltage is reversed, a new sheath adjacent to the opposite electrode begins to form in a manner similar to that of the initial sheath. Electrons released from traps in the new sheath are swept toward the old cathode (now the

[7] R. N. Dexter, J. Phys. Chem. Solids 8, 494 (1959).
[8] W. E. Spear and J. Mort, Proc. Phys. Soc. (London) 81, 130 (1963).

anode); at the edge of the initial sheath they encounter a retarding electric field and are retrapped just inside the initial sheath. Thus, for the case of a long electron range the widths of both sheaths decrease as the charge density within the new sheath increases. The process continues until (in the case of a homogeneous crystal) the new sheath becomes stationary with a constant charge density and the initial sheath disappears. The process is repeated with each voltage reversal, the only difference in the observed transient currents being due to a loss of electrons by recombination.

Details of the double sheath are algebraically complicated and are presented elsewhere.[9] Our investigations show that currents observed on half-cycles subsequent to the first are completely consistent with the above interpretation. Values obtained for the initial concentration of trapped electrons and the thermal release time as determined using the simple, single-sheath model for the first half-cycle are in close agreement with those determined by a double-sheath analysis of subsequent half-cycles. While no new information about the trapping states is made available by a double-sheath analysis, this close agreement nevertheless adds further weight to interpretations of the polarization process presented previously.

VII. SUMMARY

Experimental results presented in this paper are interpreted as arising from polarization of insulating CdS by the formation of a positively charged sheath adjacent to the negative, noninjecting electrode. This interpretation is based upon the following considerations: (1) When step voltages are applied to the optically pre-excited crystal, the transported charges increase approximately as the square root of the applied voltage. (2) When a square-wave voltage is applied to the optically pre-excited crystal, the current during each half-cycle decays to a negligibly small value, the charges transported during consecutive half-cycles are approximately the same in magnitude and they are individually much larger than the charge required to recharge the electrodes.

Evidence is also given which indicates that the sheath forms as a result of the thermal release of electrons from trapping states. The long decay time (of the order of hundreds of seconds) of the transient current and the rapid decrease in the decay time with increasing temperature are consistent with this interpretation.

The rate at which electrons recombine is much smaller than the rate at which they are retrapped. This yields the result that only a small fraction of the electrons which take part in the polarization process recombine during the life of the transient current.

Evidence is given which suggests that retrapping plays an important role in the polarization process. The range is shown to be useful in establishing the extent to which retrapping may affect the sheath formation.

Two models are presented which provide methods for analyzing transient currents which arise during polarization. An estimate of the character of trapping states (their energy distribution, concentration and time constant) may be made by employing the simple, single-sheath model. Comparison of the theory of the simple model with experimental data suggests that trapping states in the crystals investigated are concentrated at a discrete energy level. The model yields values for the initial concentration of electrons in traps and for the release rate time constant. The temperature dependence of the time constant verifies that the trapping states lie at a discrete energy level. The activation energy and frequency factor associated with the states are determined from this dependence.

Comparison of the theory of the range-limited model with experimental data provides a reliable estimate of the magnitude of the electron range. Hence, good estimates are obtained for the capture cross section and density of trapping states.

ACKNOWLEDGMENTS

The authors are indebted to Professor George Warfield for his helpful suggestions with regard to experimental procedures. Appreciation is extended to Roland W. Smith of RCA Laboratories who supplied the CdS crystals and to Steven R. Hofstein also of RCA Laboratories who helped in the fabrication of the masks used in the electrode deposition.

[9] N. F. J. Matthews and P. J. Warter, Jr., Tech. Rept. No. 7, Department of Electrical Engineering, Princeton University, 1964 (unpublished).